Desalination and Water Treatment
www.deswater.com

doi: 10.5004/dwt.2018.22654

123 (2018) 168–178
August

Application of optimal mixture design in aluminum-dolomite composite for Cr(VI) removal from aqueous solution

Yuming Peng[a], Bin Sun[a], Zhengyuan Feng[b], Nan Chen[b,c,], Jianguo Wang[b], Minghui Lv[a,*]

[a]*Shandong Provincial Geo-mineral Engineering Exploration Institute, Shandong 250014, China)*
[b]*School of Water Resources and Environment, China University of Geosciences (Beijing), Beijing 100083, China, Tel. +86 0531 81852355; Fax: +86 0531 88933178; email: chennan@cugb.edu.cn (N. Chen)*
[c] *Key Laboratory of Groundwater Cycle and Environment Evolution (China University of Geosciences (Beijing)), Ministry of Education, Beijing 100083, China*

Received 11 December 2017; Accepted 19 June 2018

ABSTRACT

An effective aluminum-dolomite composite, developed with a mixture of dolomite, bentonite, sawdust, and $AlCl_3$, has been used for Cr(VI) removal from aqueous solution. Optimal mixture design method was used to determine the optimum mixture proportions by evaluating both chromium removal efficiency and mechanical strength. It was found that the optimum adsorption capacity and strength can be achieved with the proportion of 4.90 g dolomite, 3.12 g bentonite, 1.48 g sawdust, and 0.50 g $AlCl_3$ (10 g in total). Batch experiments were carried out using the composite revealed that 92% removal efficiency for Cr(VI) was occurred at pH 6 and room temperature (20°C). The adsorption kinetic and isotherm data well agreed with the pseudo-first-order kinetic and the Freundlich isotherm models, respectively. The co-existing anions (chloride, nitrate, and acetate) had slight negligible influence, and sulfate could significantly decrease the Cr(VI) adsorption efficiency. The aluminum-dolomite composite is a cost-effective adsorbent for Cr(VI) removal from aqueous solution, especially from low-level (<50 mg/L) sulfate solution, and no secondary pollution was observed after adsorption process.

Keywords: Chromium(VI) adsorption; Aluminum-dolomite composite; Isotherms; Kinetics; Optimal mixture design (OMD)

1. Introduction

Release of chromium in aqueous solution has become a serious threat to environment and human health due to its carcinogenicity and toxicity [1]. Chromium is a primary metal pollutant in aqueous medium mainly due to anthropogenic activities (e.g., mining, leather tanning, cement, electroplating, dyeing, pesticides, and fertilizer) [2,3]. Usually, chromium exists as both trivalent and hexavalent species, while hexavalent chromium Cr(VI) is more toxic and relatively nocuous [4,5]. The detrimental health effects of Cr(VI) promoted the World Health Organization (WHO) and United States Environmental Protection Agency (USEPA) to reduce the maximum limit in drinking water from 0.05 to 0.1 mg/L [6,7]. Nevertheless, China, India, Pakistan, and some other developing countries where a high risk of Cr(VI) poisoning exists retain the former standard as the guideline for drinking water [8].

A variety of technologies are available for Cr(VI) removal from aqueous solution, such as adsorption [9], ion-exchange [10], membrane technology [11], electrodialysis [12], and photocatalytic degradation [13]. As a consequence of the consideration of cost effectiveness, high efficiency, ease in operation, and simplicity of design, adsorption is the most available method in recent decades.

Many previous researchers focused on Cr adsorption with polyvalent metal-modified natural mineral materials, activated carbon, and nanomaterials [8,14,15]. Despite such advantages as high surface area and positive charge, such

* Corresponding author.

adsorbents are still difficult to apply due to their short life expectancy, pH adjustment, and high cost of reagent [4,16]. In particular, these materials are available only as fibrous or fine powders that are difficult to separate from liquid after adsorption [17].

This study has developed a novel aluminum-dolomite composite for removing Cr(VI) from aqueous solution in order to overcome these obstacles. This composite is the solid spherical shape (D = 1–2 mm), with high Cr(VI) adsorption efficiency and strong mechanical strength to retain physical property after cyclic adsorption process. Aluminum-dolomite composite was comprised of dolomite, bentonite, sawdust, and $AlCl_3$ powder. Bentonite was used as plasticizer due to its stickiness and ability to be prepared to any shape and size. Sawdust was used to increase the porosity of the aluminum-dolomite composite after calcination. Maximization of Cr(VI) adsorption efficiency and optimization of composite mechanical strength are the factors in evaluating the adsorbent for practical applications.

The objective of this study was to prepare and investigate the aluminum-dolomite composite as a feasible chromium adsorbent. The optimal mixture design (OMD) method was used to determine the optimum proportion for Cr(VI) adsorption efficiency and mechanical strength. The effects of pH, contact time, and temperature were investigated to evaluate the performance of Cr(VI) adsorption onto aluminum-dolomite composite. Mechanisms involved in Cr(VI) adsorption were explored by combining materials characterization and adsorption performance in batch experiments.

2. Materials and methods

2.1. Materials

Dolomite and bentonite materials (below 200 mesh) were provided by Zhenyongwei Technology Development Co., Ltd. (Beijing, China). The powders were dried at 105°C for 24 h and then used for developing the composite. Sawdust (150–200 μm) was collected from wood processing factory in Changping District (Beijing, China). Potassium dichromate and $AlCl_3$ were purchased from Aladdin Industrial Co., Ltd. (Shanghai, China). Other chemical agents used were all analytical grade and all solutions were prepared with distilled water. The solution pH was adjusted with 0.1 M HCl or NaOH solutions.

2.2. Methods

2.2.1. Preparation of aluminum-dolomite composite

The aluminum-dolomite composites were made of the prepared powders (dolomite, bentonite, sawdust, and $AlCl_3$) with different proportions. Dolomite, mainly consisting of calcium and magnesium carbonate minerals, was used as aggregate of the composite. Bentonite, a common and inexpensive nonmetallic mineral, was used as binder of the adsorbent. Sawdust was taken as a porosifier to make more pores after the composites were calcined in muffle furnace. Aluminum chloride was introduced as a modifier for the content of Al, which has a good affinity with dichromate.

The prepared powders were mixed homogeneously and added with distilled water to make the desired moisture. Then, the paste was divided and kneaded into spherical granules 1–2 mm in diameter. After preparation, these samples were dried at 105°C in an oven and maintained for 24 h. The dried samples were taken out and placed in a muffle furnace. The calcination temperature was set to be 700°C and maintained for 1 h. Finally, the prepared composites were naturally cooled to room temperature for further adsorption experiments.

2.2.2. Mixture design and statistical analysis

The OMD method, provided by Design-Expert statistical software (version 8.0.6.1, Stat-Ease, Inc., Minneapolis, MN), was used to determine the optimal mixture proportion of aluminum-dolomite composites for Cr(VI) removal efficiency and mechanical strength. The OMD method can not only establish the response surface model of continuous variables, determining each component in the mixture and their interactions, but also optimize the proportion of the component according to the target [17,18]. In this study, four components had their own functions in composite production. They were defined as independent variables and designated as X_1, X_2, X_3, and X_4, respectively. Considering the advantage of low cost in using natural materials and less chemical reagent, the proportion of each component in the mixture has its restriction, $40\% \le X_1 \le 60\%$, $20\% \le X_2 \le 40\%$, $10\% \le X_3 \le 20\%$, $5\% \le X_4 \le 15\%$, in the form of $X_1 + X_2 + X_3 + X_4 = 1$. A four-component OMD consists of 2^4-1 run sheets, which are the four permutations of (+0.5, –1, +1, –1), (+1, –0.5, –1, –1), (–0.5, 0, 0, 0), and (–0.5, –0.5, 0, +1) as vertexes and interiors, respectively [19].

The OMD with the above constraint on the component proportions was ascertained in Table 1. The regression models of two responses (Y and Z) were obtained through a cubic polynomial regression fitting as given by the following equation [17]:

$$Y(\text{or } Z) = \sum_{i=1}^{n} b_i X_i + \sum_{i<j} b_{ij} X_i X_j + \sum_{i<j<k} b_{ijk} X_i X_j X_k, \ (i = 1,2,3.....n) \quad (1)$$

where Y is Cr(VI) removal efficiency (%), Z is mechanical strength of composites (Hv kgf/mm^2), X_i, X_j, and X_k are the levels of variables, b_i is the coefficient of the linear term, b_{ij} and b_{ijk} are the coefficients of the cross-product terms, and n is the number variables. The analysis of variance (ANOVA) of Eq. (1) was generated by Design-Expert software (shown in Table 2), and the regression coefficients were then used to generate contour plots for determining the optimum region for each response.

2.2.3. Characterization analysis

The surface morphology of aluminum-dolomite composites were carried out using the scanning electron microscope (SEM) (SHIMADZU SSX-550, Japan). Composites were freeze fractured, using liquid N_2 to produce a clean brittle fracture, and were subsequently sputter-coated with Au before SEM observation. The specific surface areas of composites were determined by the Brunauer–Emmett–Teller (BET) method with N_2 adsorption (Coulter SA3100, USA). Mechanical strength was tested using a Micro Vickers

Table 1
Experimental variables and responses used in the optimal mixture design (OMD)

Run	Actual values				Coded values				Response	
	X_1 (g) (dolomite)	X_2 (g) (bentonite)	X_3 (g) (sawdust)	X_4 (g) ($AlCl_3$)	X_1 (g) (dolomite)	X_2 (g) (bentonite)	X_3 (g) (sawdust)	X_4 (g) ($AlCl_3$)	Y (%) (removal efficiency)	Z (Hv) (kgf/mm^2) (mechanical strength)
1	4.5	2.0	2.0	1.5	–0.5	–1	0	+1	20.5	7.4
2	4.5	4.0	1.0	0.5	–0.5	+1	–1	–1	84.5	12.0
3	4.0	3.5	1.0	1.5	–1	+0.5	–1	+1	51.2	11.0
4	5.5	2.0	1.5	1.0	+0.5	–1	0	0	88.1	10.2
5	5.5	2.0	2.0	0.5	+0.5	–1	+1	–1	91.2	8.5
6	4.0	3.0	2.0	1.0	–1	0	+1	0	73.5	9.8
7	4.5	3.0	1.5	1.0	–0.5	0	0	0	65.4	10.0
8	4.5	2.5	1.5	1.5	–0.5	–0.5	0	+1	78.0	10.1
9	5.5	2.0	1.0	1.5	+0.5	–1	–1	+1	74.5	9.7
10	5.0	3.0	1.0	1.0	0	0	–1	0	85.1	10.5
11	6.0	2.5	1.0	0.5	+1	–0.5	–1	–1	86.5	10.2
12	5.5	2.5	1.5	0.5	+0.5	–0.5	0	–1	90.2	10.8
13	4.5	2.5	2.0	1.0	–0.5	–0.5	1	0	87.8	9.6
14	5.0	3.0	1.5	0.5	0	0	0	–1	94.0	10.5
15	5.0	3.5	1.0	0.5	0	+0.5	–1	–1	88.4	12.5

Table 2
ANOVA for Cr(VI) removal efficiency and mechanical strength calculated from the optimal mixture design (OMD)

Response	Source	DF (Degree of freedom)	Sum of squares	Mean square	F-Value	P-Value
Y (%) (removal efficiency)	Regression	13	6,153.48	473.34	222.71	<0.0001
	Linear	3	4,038.28	1,346.09	633.33	<0.0001
	Residual error	6	12.75	2.13		
	Lack of fit	1	12.75	12.75		
	Pure error	5	0.00	0.00		
	Cor total	19	6,166.24			
Z (Hv) (kgf/mm^2) (mechanical strength)	Regression	13	24.34	1.87	14.26	<0.0001
	Linear	3	19.52	6.51	18.55	<0.0001
	Residual error	16	5.61	0.35		
	Lack of fit	11	5.61	0.51		
	Pure error	5	0.00	0.00		
	Cor total	19	25.13			

hardness testing machine (AKASHI MVK-E, Japan). Fourier transform infrared (FTIR) spectroscopy (Vertex 70V, Bruker, Germany) was used to determine the surface functional groups change in the adsorbent before and after Cr(VI) adsorption. The crystallinity of the aluminum-dolomite composites was identified by X-ray powder diffraction (XRD) (D/max-2500, Rigaku, Tokyo, Japan) with Cu-Kα radiation (λ = 1.54056 Å). Moreover, powdered samples were directly analyzed without pretreatment. Chromium(VI) concentration in the solution was determined with a UV-visible spectrophotometer (HACH DR/6000, USA). A digital standard pH meter was used for pH measurements (ORION 8157BNUMD, USA). The leached aluminum was analyzed by inductively coupled plasma optical emission spectrometry (THERMO ICAP6300, USA).

2.2.4. Batch adsorption experiments

Batch adsorption experiments were performed to obtain kinetic and equilibrium data. For kinetic study, 100 mL synthetic Cr(VI) solutions with initial concentrations of 10 and 50 mg/L were loaded into a 250 mL glass-stoppered conical flask, respectively. The adsorption process was carried out with a dosage of 10 g/L at room temperature (25°C ± 2°C).

Samples were taken at a constant interval and filtered through a 0.45 μm nylon membrane filter to measure the Cr(VI) concentration. The adsorption equilibrium isotherm parameters of the process were obtained via the addition of 10 g/L of the composites into 100 mL of various initial Cr(VI) concentrations (10, 30, 50, 75, 100, and 150 mg/L) at different (10°C, 20°C, 30°C, and 40°C) temperatures.

The experiments of pH effect on Cr(VI) adsorption were tested by using 100 mL Cr(VI) solutions at room temperature. The initial solution pH values ranged from 2 to 11 by using 0.1 M NaOH or HCl solution to achieve the desired value. In order to identify the effects of co-existing anions on Cr(VI) adsorption, the adsorptions were carried out using Cr(VI) solutions of 10 mg/L containing 10, 20, 50, 100, and 200 mg/L of anions, including Cl^-, NO_3^-, CH_3COO^-, SO_4^{2-}, and S^{2-}.

Each test was conducted in duplicate and averaged results were reported. The amount of Cr(VI) adsorbed was calculated using the following equation:

$$q_t = \frac{(C_0 - C_e)V}{m} \quad (2)$$

where C_0 and C_e are the initial and equilibrium Cr(VI) concentrations (mg/L), respectively, V is the volume of the aqueous solution (L), and m is the adsorbent mass (g).

3. Results and discussion

3.1. Analysis of the OMD model

The data in Table 1 were used to fit the polynomial model representing the responses (Y and Z) as a function of dolomite, bentonite, sawdust, and $AlCl_3$. The following two equations express the overall predictive models in terms of the coded variables:

$$\begin{aligned} Y = {} & 68.7053X_1 - 31.5162X_2 + 541.4003X_3 + 1,233.2502X_4 \\ & - 4.1470X_1X_2 - 108.1631X_1X_3 - 243.8299X_1X_4 - 1.8094X_2X_3 \\ & - 135.5795X_2X_4 - 806.4881X_3X_4 - 1.5517X_1X_2X_3 \\ & + 24.8391X_1X_2X_4 + 151.4744X_1X_3X_4 - 1.4569X_2X_3X_4 \end{aligned} \quad (3)$$

with adj $R^2 = 0.997$.

$$\begin{aligned} Z = {} & -2.9836X_1 - 9.5782X_2 + 7.4659X_3 + 10.8465X_4 \\ & + 3.4880X_1X_2 - 0.72651X_1X_3 + 0.5319X_1X_4 + 1.2077X_2X_3 \\ & + 9.5216X_2X_4 - 30.7287X_3X_4 - 0.4489X_1X_2X_3 \\ & - 2.9780X_1X_2X_4 + 5.4688X_1X_3X_4 + 2.2999X_2X_3X_4 \end{aligned} \quad (4)$$

with adj $R^2 = 0.998$. The adequacy of the regression model for explaining the experiment at a 95% confidence level was tested by ANOVA results. The ANOVA includes some statistic factors such as lack of fit, R^2, and adjusted R^2. The ANOVA results (Table 2) indicated that the model was highly significant, as P-value for the model was <0.0001. The value of adjusted R^2, a measurement for fitness of the regressed Eq. (3), was 0.997, and that of Eq. (4) was 0.998. These results indicated that the models obtained were able to give a good estimate of response of the system in the studied range. The calculated F-values were 222.71 and 14.26, demonstrating that most of the variables in the response can be explained by the regression equations [20]. In Eq. (3), three of the variables (X_1, X_3, and X_4) had positive effects on Cr(VI) removal, but the value of $X_4 > X_3 > X_1$ demonstrated that the linear term influence of X_4 was more significant than that of X_1 and X_3, indicating that the amount of $AlCl_3$ was the main factor influencing Cr(VI) removal. Fig. 1 shows a comparison between predicted and actual values of the Cr(VI) removal efficiency and mechanical strength by using the resulted polynomial Eqs. (3) and (4). This plot confirms that the actual values are in good agreement with the predicted values.

3.1.1. Mixture contour plots and responses

The mixture contour plots of the two responses are shown in Fig. 2 to present more detailed interactions related to the regression models on Cr(VI) removal efficiency and mechanical strength. The plots gave three variations of interactions on the responses ($AlCl_3$ = 0.500, 1.000, and 1.500, respectively), and the darker red areas represent the higher Cr(VI) removal efficiency and mechanical strength. Chromium(VI) removal increased with increasing dolomite and decreasing $AlCl_3$ proportions, while bentonite and sawdust amount did not significantly influence the Cr(VI) adsorption. Nevertheless, increasing the ratios of bentonite and decreasing the ratios of sawdust would improve the mechanical strength. The lowest mechanical strength was found in the highest mass ratio of sawdust (20%) and $AlCl_3$ (15%), as well as the lowest ratio of bentonite (20%).

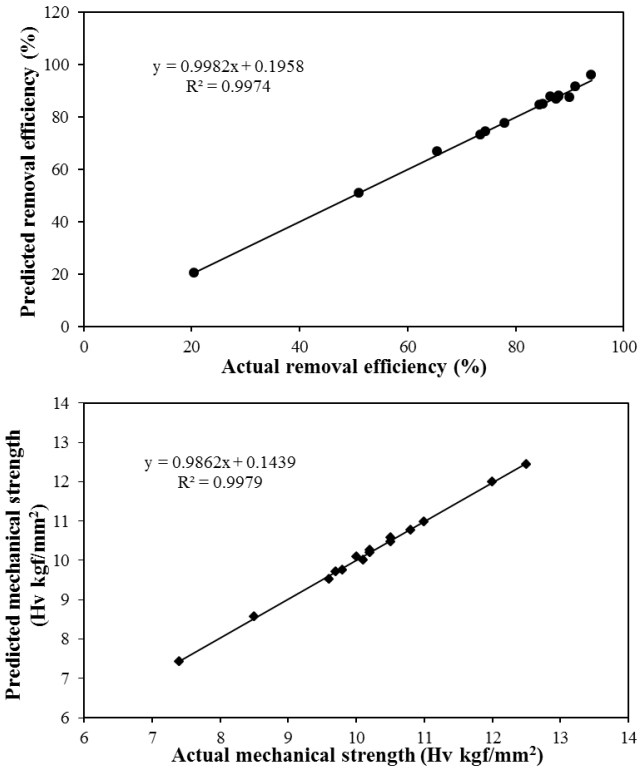

Fig. 1. Plot of predicted results of Cr(VI) removal efficiency and mechanical strength versus actual (experimental) values.

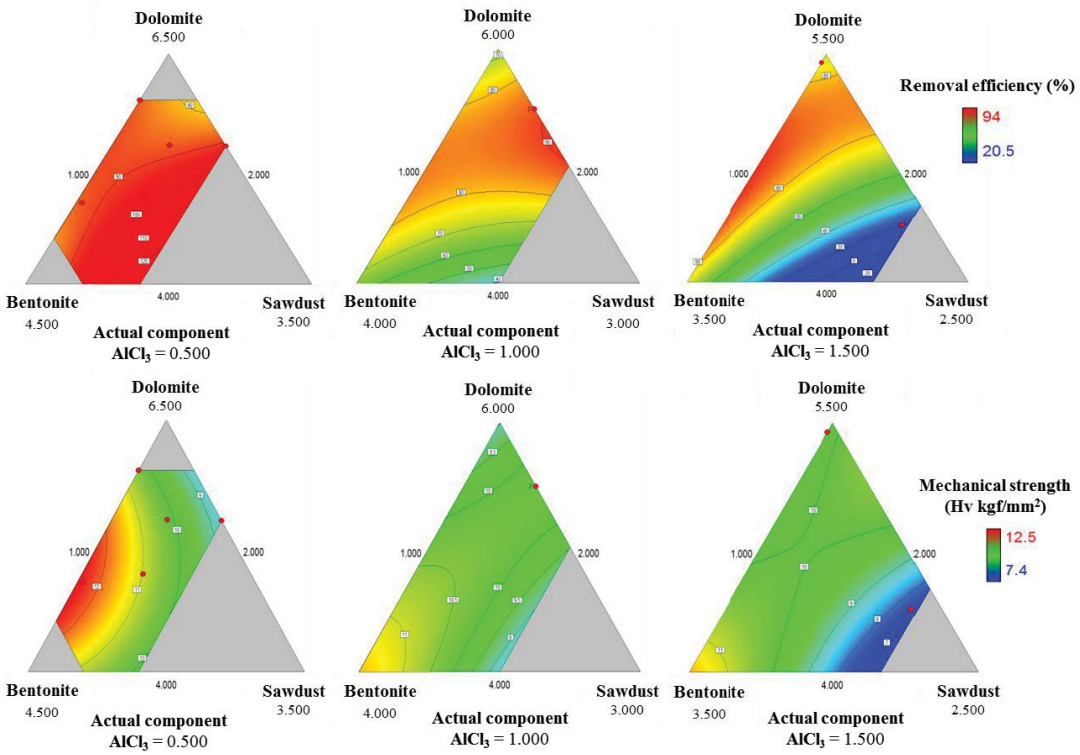

Fig. 2. Triangular-dimensional contour plots and responses for the effect of dolomite (X_1), bentonite (X_2), sawdust (X_3), and $AlCl_3$ (X_4) on Cr(VI) removal efficiency and mechanical strength.

3.1.2. Optimization of mixing proportion for responses

Considering the significant differences in the optimum proportions for Cr(VI) removal and mechanical strength, a response optimizer was used to determine the optimum proportions to meet the expectations of both responses. The optimizer started from a constant composition and terminated when the target response values were obtained. The optimization contour and 3D surface plots (Fig. 3) depict that the optimum proportion of each component in a 10 g mixture was 4.90 g of dolomite, 3.12 g of bentonite, 1.48 g of sawdust, and 0.50 g of $AlCl_3$. The predicted responses for Cr(VI) removal efficiency and mechanical strength were 95.09% and 10.7 Hv with a high composite desirability of 1.000.

An experiment with the optimized composite was conducted to gain the validity of OMD model. The results identified that the actual data (94.2% and 10.3 Hv) were in a good agreement with the predicted values. Further batch experiments were carried out by using the aluminum-dolomite composite with the optimum proportions.

3.2. Characterization of aluminum-dolomite composite

In order to obtain more insight into the Cr(VI) removal process, SEM and BET analytical technologies were employed.

The prepared aluminum-dolomite composite is grayish-white colored, spherical particulate and 1–2 mm in

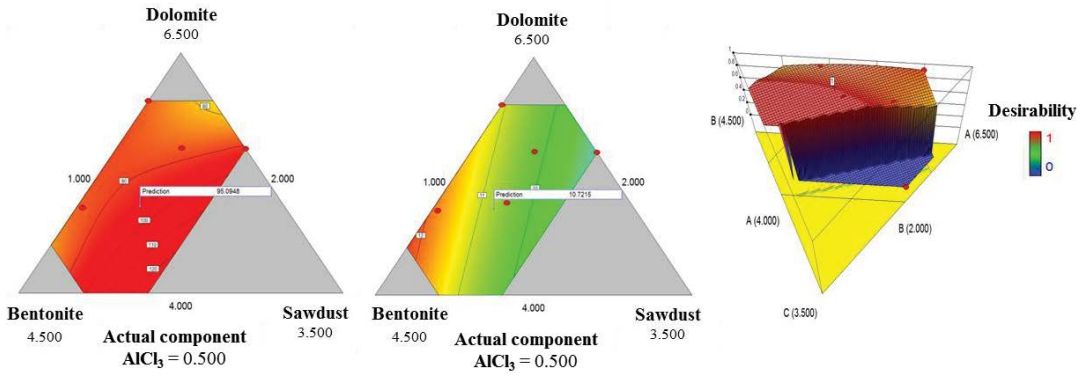

Fig. 3. Optimization mixing proportion and composite desirability for responses of Cr(VI) removal efficiency and mechanical strength based on the OMD.

diameter (Fig. 4(a)). SEM images of pristine and saturated aluminum-dolomite composites at the same magnification (1,000×) are shown in Figs. 4(b) and (c). The pristine composite (Fig. 4(a)) exhibited irregular large amounts of porous structures (10–20 μm in diameter), which indicates the composite may have a high adsorption capacity. These micron grade pore structures can be explained by the sintering of inorganic and organic substances in natural mineral materials and sawdust during the calcination process [21]. Conversely, the adsorbed composite (Fig. 4(c)) appeared to be slice state and scalelike, which would be attributed to the formation of new chromium crystalline complexes on the surface of adsorbent.

The BET surface area of aluminum-dolomite composite was found to be 37.83 m^2/g. The corresponding pore volume and average pore diameter were 0.0610 cm^3/g and 15.20 nm, respectively. The typical nitrogen adsorption–desorption isotherm for the aluminum-dolomite composite is shown in Fig. 4(d). The composites displayed a type IV isotherm model according to International Union of Pure and Applied Chemistry (IUPAC) classification [22]. A small H2-type hysteresis loop was observed in the range of 0.3–0.9, indicating the presence of ink-bottle pores with narrow necks. Meanwhile, at high relative pressure between 0.9 and 1.0, the shape of hysteresis loops resembles type H3, which is associated with slit-like pores [23]. In addition, the observed hysteresis loop shifted to a higher relative pressure ($P/P_0 > 0.9$) was due to increase in the nitrogen adsorption in macropores [22].

XRD data obtained from the aluminum-dolomite composite were analyzed by the software of Search Match and the patterns are shown in Fig. 5. As can be seen from Fig. 5, the composition of the aluminum-dolomite composite is $Mg_{0.06}Ca_{0.94}CO_3$, $(Al(OH)_2)_{0.33}Al_2(Si_{3.67}Al_{0.03}O_{10})(OH)_2$, and $AlCl_3$.

The FTIR spectra were obtained to get the information on the structural changes of the aluminum-dolomite composite before and after Cr(VI) adsorption (Fig. 6). The band at 876 cm^{-1} was the characteristic dolomite band [24]. The bands around 1,437 and 3,435 cm^{-1} were related to the presence of hydroxyl groups (OH) and HCO_3^- group, respectively [25]. The band at 2,974 cm^{-1} was assigned to carbonates [26]. There were two new bands around 2,520 and 3,702 cm^{-1} after Cr(VI) adsorption. The band at 2,520 cm^{-1} was due to the presence of carbonates [26]. The band at 3,702 cm^{-1} was assigned to –OH [27]. Thus, those demonstrated that Cr(VI) could be immobilized well onto the aluminum-dolomite composite due to the chemical reaction.

3.3. Batch adsorption experiments

3.3.1. Kinetic study

Kinetic study was carried out under the described conditions in Section 2.2.4 for 6 h per sample until the equilibrium was achieved. Chromium(VI) uptake at any time q_t (mg/g) was calculated using Eq. (2). Pseudo-first-order and pseudo-second-order kinetics were applied to study the kinetics of

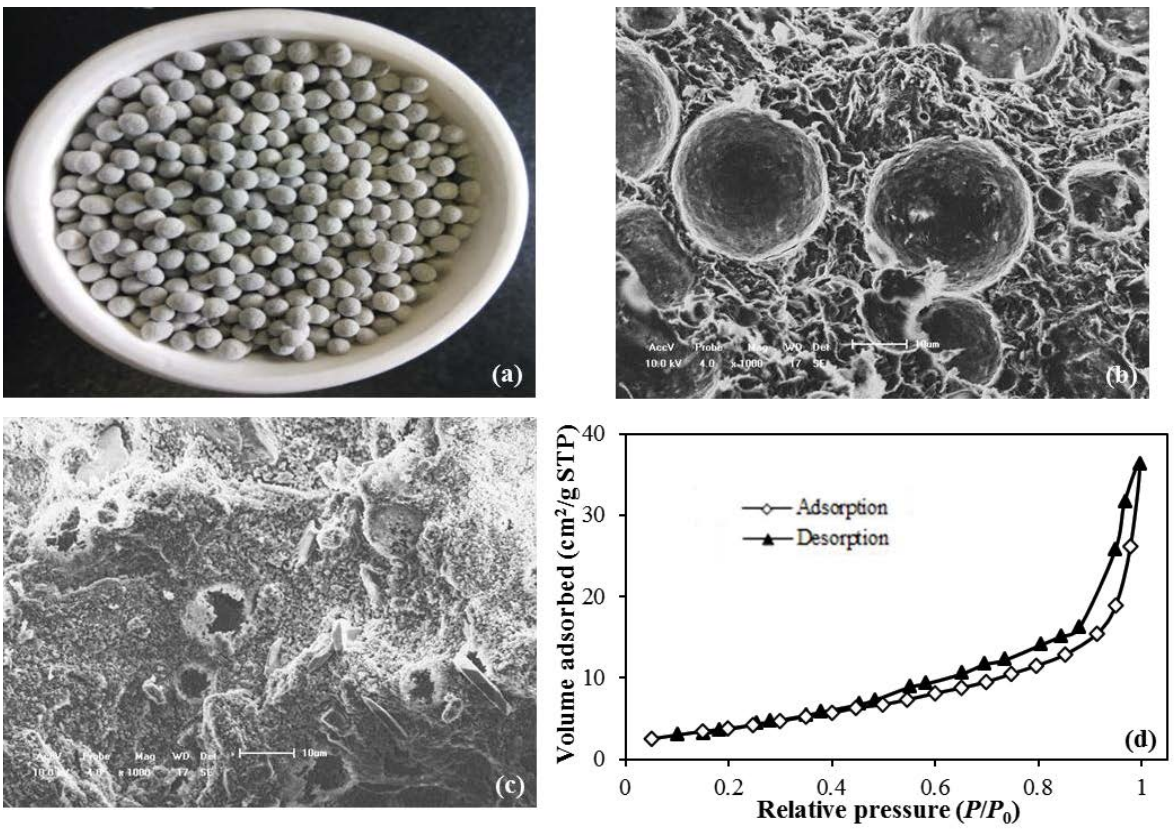

Fig. 4. Photo of the aluminum-dolomite composite (a), SEM images (1,000×) of pristine composite (b) and adsorbed composite (c), nitrogen adsorption–desorption isotherm of composite (d).

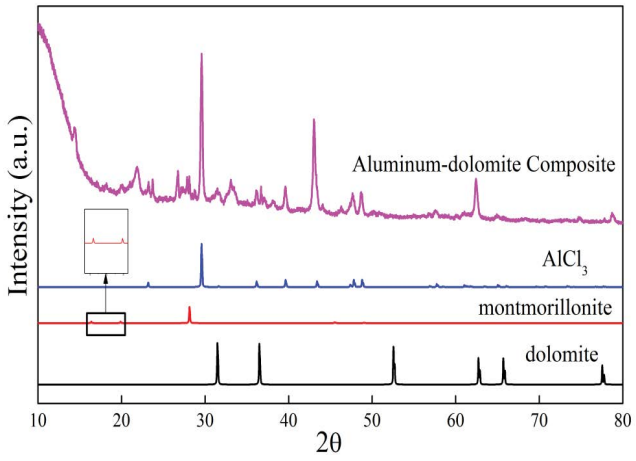

Fig. 5. XRD patterns of the aluminum-dolomite composite.

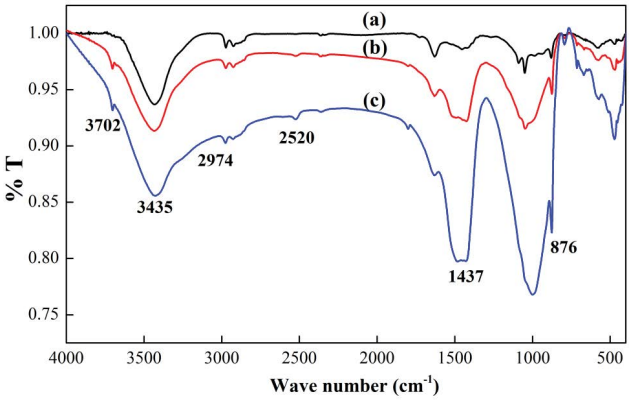

Fig. 6. FTIR spectra of the aluminum-dolomite composite (a), Cr(VI)-laden aluminum-dolomite composite (10 mg/L) (b), and Cr(VI)-laden aluminum-dolomite composite (50 mg/L) (c).

Cr(VI) adsorption process by using the nonlinear model as following equations (Fig. 7(a)) [28,29]:

$$q_t = q_e[1-\exp(-k_1 t)] \tag{5}$$

$$q_t = \frac{q_e^2 K_2 t}{1+q_e K_2 t} \tag{6}$$

where q_e and q_t (mg/g) are the amount of adsorbate adsorbed at equilibrium and at any time t (h), respectively, k_1 is the pseudo-first-order kinetic rate constant (h^{-1}), and k_2 is the pseudo-second-order kinetic rate constant (g/mg h).

The model constants and the correlation coefficients (R^2) are presented in Table 3. The pseudo-first-order rate equation was found to better explain the data compared with the pseudo-second-order equation, suggesting that the Cr(VI) adsorption process onto aluminum-dolomite composite was more inclined to physical adsorption [30]. The equilibrium adsorption capacity calculated from pseudo-first-order model was 0.997 mg/g (initial concentration of 10 mg/L), which was closer to the experimental value (0.923 mg/g). Besides, the adsorption rate constant k_1 value was found to be 0.044 and 0.037 g/h at the initial concentration of 10 and 50 mg/L, respectively.

3.3.2. Adsorption isotherms

The adsorption equilibrium isotherm models would help to reveal the Cr(VI) adsorption mechanism, the surface properties, and affinity of the adsorbent. In this study, the Langmuir and Freundlich isotherm models were established to describe the dynamic balance on solid and liquid interface.

The Langmuir model is based on the hypothesis that uptake occurs on a homogenous surface by monolayer adsorption without interaction between adsorbed molecules. The nonlinear Langmuir equation is expressed as follows [31]:

$$q_t = \frac{K_L q_{\max} C_e}{1+K_L C_e} \tag{7}$$

where q_e and $q_{\max}$ represents the equilibrium and maximum adsorption capacity (mg/g), C_e is the equilibrium Cr(VI) concentration in the solution (mg/L), and K_L is the adsorption intensity related to the adsorption energy (L/mg).

The Freundlich isotherm model is based on the assumption that the adsorbent surface energy is heterogeneous and adsorption is multilayered. The nonlinear Freundlich equation is expressed as follows [25]:

$$q_e = K_F C_e^{1/n} \tag{8}$$

where K_F ((mg/g)(L/mg)$^{1/n}$) provides an indication of the adsorption capacity (mg/g) and n is related to the intensity of adsorption.

The values of K_L, $q_{\max}$, K_F, n, and correction coefficients (R^2) were shown in Table 3, while the plot of Freundlich isotherm model of Cr(VI) removal on the composite at different temperatures was displayed in Fig. 7(b). It can be seen from the data that the Freundlich isotherm yields a better fit to the experimental data by evaluating the correlation coefficient values than the Langmuir isotherm. The fact indicates that Cr(VI) adsorption process is multilayered and nonhomogeneous. The Freundlich parameter, n, was estimated as 2.290, 2.702, 2.279, and 2.375 (<10.000), which confirms that Cr(VI) adsorption by aluminum-dolomite composite was favorable. The $q_{\max}$ was 4.586 mg/g at 20°C and 7.695 mg/g at 30°C, respectively.

3.3.3. Adsorption thermodynamics

The thermodynamic parameters are related to the adsorption action. Generally, the standard of Gibbs free energy ΔG, entropy and enthalpy change ΔS and ΔH can be expressed by the following equations [32]:

$$K_d = \frac{(C_0 - C_e)\times V}{mC_e} \tag{9}$$

$$\ln K_d = \frac{-\Delta G}{RT} \tag{10}$$

$$\Delta G = \Delta H - T\Delta S \tag{11}$$

where K_d is the distribution coefficient, m is the dosage of adsorbent (g), R is the gas constant, and T is the Kelvin temperature. The calculated values of ΔH, ΔS, and ΔG for the

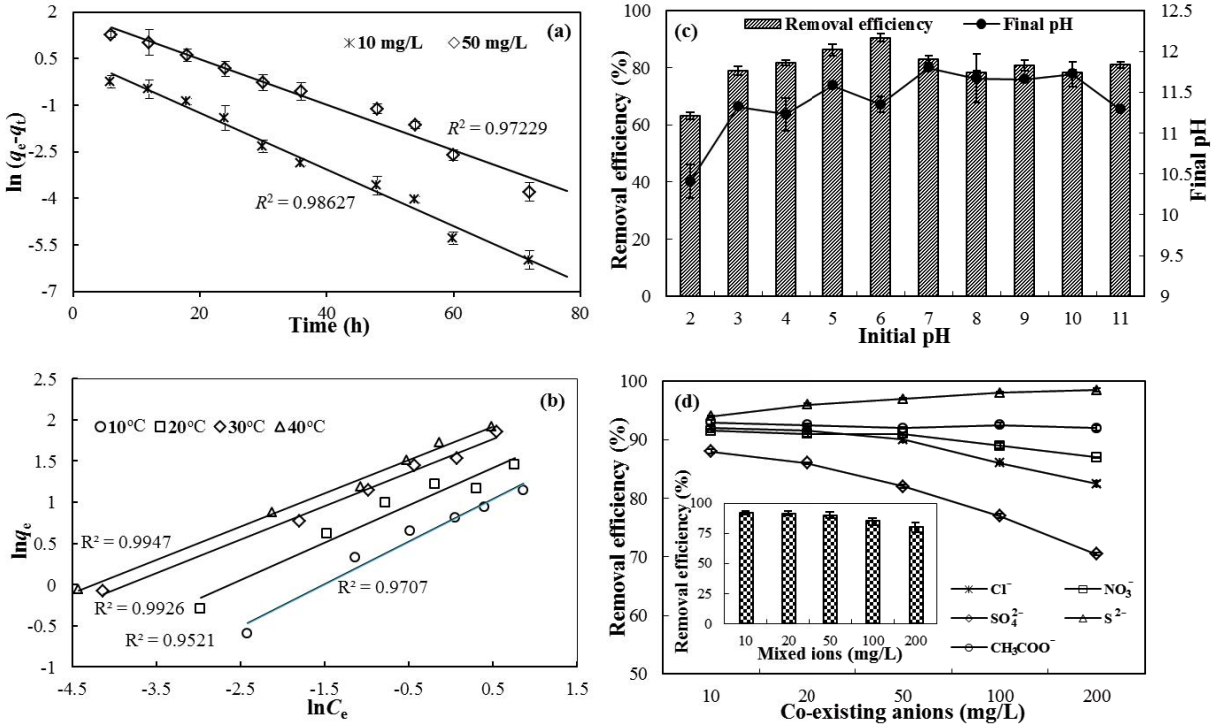

Fig. 7. Plot of pseudo-first-order model of the removal of Cr(VI) by the aluminum-dolomite composite (a), plot of Freundlich isotherm model of Cr(VI) removal on the composite (b), effect of pH (2.0–11.0) on the removal of Cr(VI) by the composite (c), and effects of co-existing anions and mixed ions on Cr(VI) adsorption (d).

Table 3
The constant parameters of kinetic and isotherm models for Cr(VI) adsorption onto the aluminum-dolomite composite

Concentration (mg/L)	Pseudo-first-order kinetic			Pseudo-second-order kinetic		
	k_1 (g/h)	q_e (mg/g)	R^2	k_2 (g/mg h)	q_e (mg/g)	R^2
10	0.044	0.997	0.946	0.029	1.328	0.917
50	0.037	4.293	0.956	0.005	5.946	0.937
Temperature (°C)	Langmuir isotherm			Freundlich isotherm		
	q_{max} (mg/g)	K_L (L/mg)	R^2	n	K_F (mg/g)(L/mg)$^{1/n}$	R^2
10	3.730	0.034	0.979	2.290	0.395	0.979
20	4.586	0.061	0.943	2.702	0.760	0.925
30	7.695	0.038	0.923	2.279	0.872	0.981
40	8.465	0.439	0.936	2.375	1.082	0.989

adsorption of Cr(VI) onto the composite material are listed in Table 4. The obtained positive ΔH values indicated endothermic nature of Cr(VI) adsorption. The positive values of ΔS reflected increased randomness at the solid/solution interface in the course of removal. Negative values of ΔG confirmed that Cr(VI) adsorption onto the composite was spontaneous.

3.3.4. Effect of pH

The effect of pH on Cr(VI) removal from aqueous solution is presented in Fig. 7(c). The optimal value for Cr(VI) uptakes appeared at pH 6, with a removal efficiency of 92%. The removal ability fluctuated slightly in the pH range of 3–11, indicating that the composite could adapt to a wide range of pH for Cr(VI) adsorption and was suitable for practical application in industrial conditions. The decrease of adsorption efficiency at pH < 3 was mainly due to the adsorbent loss caused by the solubilization and degradation [17]. The speciation of Cr(VI) in aqueous solution as a function of pH was obtained from Visual MINTEQ results (Fig. 8). It could be found that $HCrO_4^-$ was the main ionic form at pH 2.00–6.50, while CrO_4^{2-} was predominant in the range of pH > 6.50. The final pH changed from 10.05 to 12.00, with the initial pH increased from 2.00 to 11.00. Therefore, $HCrO_4^-$ and

Table 4
Thermodynamic parameters for Cr(VI) removal onto the composite at the initial concentration varying from 10, 30, and 50 mg/L, dosage of 10 g/L

Concentration (mg/L)	ΔH (kJ/mol)	ΔS (J/mol K)	ΔG (kJ/mol)		
			293 K	303 K	313 K
10	65.81	0.23	–2.61	–6.15	–7.16
30	32.97	0.12	–1.19	–2.24	–3.61
50	27.18	0.09	–0.38	–1.29	–1.67

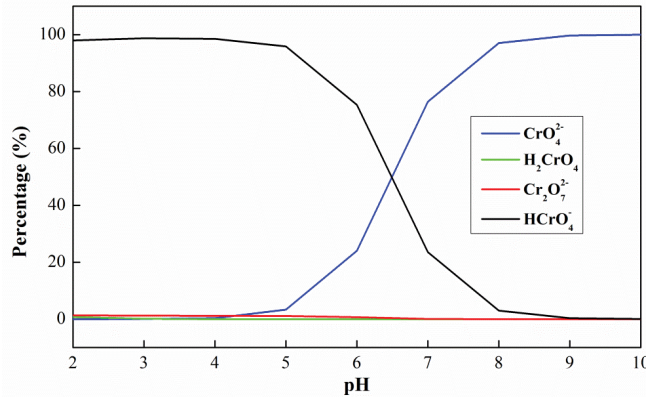

Fig. 8. Cr(VI) speciation simulated using Visual MINTEQ (Version 3.0) (Cr(VI) concentration = 10.0 mg/L, the temperature = 25°C ± 2°C).

CrO_4^{2-} were the main ions with the initial pH ranged from 2.00 to 6.50, and CrO_4^{2-} was the main ion in the initial pH > 6.50. As shown in Fig. 7(c), the point of zero charge was determined as 11.5 according to the method reported by Chen et al. [21]. Therefore, the surface characteristic of the composite is positive at pH_f < 11.5, neutral at 11.5, and negative at pH_f > 11.5. In addition, the positively charged surface sites formed on the composite can favor the adsorption of $HCrO_4^-$ as a result of electrostatic attraction with decreased pH. Conversely, the increased concentration of OH^- would compete with CrO_4^{2-} at pH above 11.5.

3.3.5. Effect of co-existing anions

The effect of co-existing anions was presented in Fig. 7(d), the presence of chloride, nitrate, and acetate ions did not significantly affect Cr(VI) removal even at a high concentration of 200 mg/L. Sulfur ion can obviously promote the Cr(VI) removal efficiency to be 98.5%, when the concentration is 200 mg/L. The surface of adsorbent turned to be green (trivalent chromium), which indicated that the reduction reaction occurred between sulfur and hexavalent chromium ions. However, sulfate ion exhibited great adverse effect, and the removal efficiency dramatically decreased from 92% to 70.5% with an increase of sulfate concentration from 0 to 200 mg/L. This phenomenon suggested that some adsorption sites on the surface of composite could be occupied by both Cr(VI) and sulfate. In addition, sulfate has two negative charges, indicating that it would have a strong electrostatic attraction with the surface of composite. Zhao et al. [9] reported that sulfate inhibited Cr(VI) removal due to competition between chromium and sulfate species. There are a large number of co-existing ions in industrial wastewater. Therefore, we simulated the industrial wastewater, including Cl^-, NO_3^-, CH_3COO^-, SO_4^{2-}, and NH_4^+ (S^{2-} was not included), to do the experiments in the laboratory scale. As shown in Fig. 7(d), the Cr(VI) removal efficiency decreased from 92% to 80% with the increased concentration of mixed ions from 10 to 200 mg/L. The above results indicated that the aluminum-dolomite composite prepared in this study can be potentially applied to the Cr(VI) pollution in industrial wastewater in a certain range.

3.3.6. Comparison of Cr(VI) adsorption capacities of various mineral adsorbents

The adsorption capacity of the synthesized composite in this study was compared with other mineral adsorbents reported in literatures as shown in w 5. It was difficult to make a direct comparison with other adsorbents reported in the literature because of the different operating conditions such as pH, temperature, and initial concentration. But a major point worth noting was that the capacity of aluminum-dolomite composite for Cr(VI) removal was considerably higher as compared with other reported mineral adsorbents, thus demonstrating the application possibility of this synthesized composite.

Table 5
Summary of Cr(VI) adsorption capacities of various mineral adsorbents

Adsorbent	Temperature (°C)	q_{max} (mg/g)	References
Raw dolomite	20	10.01	[25]
	30	8.39	
Bentonite clay	50	5.90	[33]
Dolomite–montmorillonite–corn stover composite	20	1.15	[4]
Calcined bauxite	30	2.00	[34]
Fe(III)-coated natural zeolite	23	0.082	[35]
Surfactant-modified montmorillonite clay	25	0.041	[36]
Aluminum-dolomite composite	20	4.586	This work
	30	7.695	

4. Conclusions

The predicted values of Cr(VI) removal efficiency and mechanical strength obtained using the OMD method were in good agreement with the experimental data, demonstrating that it is a favorable method for determining the optimum mixture proportion. The ANOVA result indicated that the proportion of $AlCl_3$ is positively related to Cr(VI) removal efficiency and sawdust has negative effect on mechanical strength.

The prepared aluminum-dolomite composite is an effective, solid-phase adsorbent for Cr(VI) removal under practical conditions (room temperature, wide pH range, and anticlogging characteristic), and almost no toxic sludge or leached metal ions can be observed. The Cr(VI) adsorption capacity on composite, estimated by the Langmuir equation, was 4.69 mg/g. The presence of chloride, nitrate, and acetate had slight effect on Cr(VI) removal, while sulfate can significantly decrease Cr(VI) adsorption. The pseudo-first-order kinetic model and the Freundlich isotherm equation were suitable for Cr(VI) adsorption onto aluminum-dolomite composite. The excellent Cr(VI) removal performance in the mixed ions solution of the aluminum-dolomite composite suggested it would be used in practical wastewater treatment.

Acknowledgment

The authors acknowledge financial supports from the National Natural Science Foundation of China (NSFC) (no. 21407129).

References

[1] R.A. Gil, S. Cerutti, J.A. Gásquez, R.A. Olsina, L.D. Martinez, Preconcentration and speciation of chromium in drinking water samples by coupling of on-line sorption on activated carbon to ETAAS determination, Talanta, 68 (2006) 1065–1070.
[2] N.K. Hamadi, X.D. Chen, M.M. Farida, M.G.Q. Lub, Adsorption kinetics for the removal of chromium (VI) from aqueous solution by adsorbents derived from used tyres and sawdust, Chem. Eng. J., 84 (2001) 95–105.
[3] M. Erdem, H.S. Altundoğan, F. Tümen, Removal of hexavalent chromium by using heat-activated bauxite, Miner. Eng., 17 (2004) 1045–1052.
[4] Q.Y. Wang, N. Chen, Y. Yu, C.P. Feng, Q. Ning, W.W. Hu, Chromium (VI) removal from aqueous solution using a new synthesized adsorbent, Desal. Wat. Treat., 57 (2014) 1–11.
[5] J.G. Zhou, Y.F. Wang, J.T. Wang, W.M. Qiao, D.H. Long, L.C. Ling, Effective removal of hexavalent chromium from aqueous solutions by adsorption on mesoporous carbon microspheres, J. Colloid Interface Sci., 462 (2016) 200–207.
[6] Guidelines for Drinking-Water Quality, 4th ed., World Health Organisation, Geneva, 2011.
[7] Draft Manual of Practice Identification of Illicit Connections, U.S. EPA Permits Division, 1990.
[8] Z. Liu, L. Chen, L. Zhang, S. Poyraz, Z. Guo, X. Zhang, J. Zhu, Ultrafast Cr (VI) removal from polluted water by microwave synthesized iron oxide submicron wires, Chem. Commun., 50 (2014) 8036–8039.
[9] Y.X. Zhao, S.J. Yang, D.H. Ding, J. Chen, Y.N. Yang, Z.F. Lei, C.P. Feng, Z.Y. Zhang, Effective adsorption of Cr (VI) from aqueous solution using natural Akadama clay, J. Colloid Interface Sci., 395 (2013) 198–204.
[10] S. Rengaraj, K.H. Yeon, S.H. Moon, Removal of chromium from water and wastewater by ion exchange resins, J. Hazard. Mater., 87 (2001) 273–287.
[11] A. Hafiane, D. Lemordant, M. Dhahbi, Removal of hexavalent chromium by nanofiltration, Desalination, 130 (2000) 305–312.
[12] C.S. Peng, H. Meng, S.X. Song, S.C. Lu, A.L. Valdivieso, Elimination of Cr(VI) from electroplating wastewater by electrodialysis following chemical precipitation, Sep. Sci. Technol., 39 (2005) 1501–1517.
[13] J.J. Testa, M.A. Grela, M.I. Litter, Heterogeneous photocatalytic reduction of chromium (VI) over TiO_2 particles in the presence of oxalate: involvement of Cr (V) species, Environ. Sci. Technol., 38 (2004) 1589–1594.
[14] A.B. Albadarin, C. Mangwandi, A.H. Al-Muhtaseb, G.M. Walker, S.J. Allen, M.N.M. Ahmad, Kinetic and thermodynamics of chromium ions adsorption onto low cost dolomite adsorbent, Chem. Eng. J., 179 (2012) 193–202.
[15] F. Di Natale, A. Erto, A. Lancia, D. Musmarra, Equilibrium and dynamic study on hexavalent chromium adsorption onto activated carbon, J. Hazard. Mater., 281 (2015) 47–55.
[16] S. Kushwaha, B. Sreedhar, P.P. Sudhakar, A spectroscopic study for understanding the speciation of Cr on palm shell based adsorbents and their application for the remediation of chrome plating effluents, Bioresour. Technol., 116 (2012) 15–23.
[17] R.Z. Chen, Z.Y. Zhang, C.P. Feng, K. Hu, M. Li, Y. Li, K. Shimizu, N. Chen, N. Sugiura, Application of simplex-centroid mixture design in developing and optimizing ceramic adsorbent for As (V) removal from water solution, Microporous Mesoporous Mater., 131 (2010) 115–121.
[18] A. Mirmohseni, M.S. Seyed Dorraji, A. Figoli, F. Tasselli, Chitosan hollow fibers as effective biosorbent toward dye: preparation and modeling, Bioresour. Technol., 121 (2012) 212–220.
[19] R.H. Myers, D.C. Montgomery, Response surface methodology: process and product optimization using designed experiments, J. Stat. Plan. Infer., 59 (1997) 185–186
[20] O. Prakash, M. Talat, S.H. Hasan, R.K. Pandey, Factorial design for the optimization of enzymatic detection of cadmium in aqueous solution using immobilized urease from vegetable waste, Bioresour. Technol., 99 (2008) 7565–7572.
[21] N. Chen, Z.Y. Zhang, C.P. Feng, D.R. Zhu, Y.N. Yang, N. Sugiura, Preparation and characterization of porous granular ceramic containing dispersed aluminum and iron oxides as adsorbents for fluoride removal from aqueous solution, J. Hazard. Mater., 186 (2011) 863–868.
[22] G. Leofanti, M. Padovan, G. Tozzola, B. Venturelli, Surface area and pore texture of catalysts, Catal. Today, 90 (1994) 207–219.
[23] J.B. Zhou, S.L. Yang, J.G. Yu, Z. Shu, Novel hollow microspheres of hierarchical zinc-aluminum layered double hydroxides and their enhanced adsorption capacity for phosphate in water, J. Hazard. Mater., 192 (2011) 1114–1121.
[24] S. Gunasekaran, G. Anblagan, Thermal decomposition of natural dolomite, Bull. Mater. Sci., 30 (2007) 339–344.
[25] A.B. Albadarin, C. Mangwandi, H. Ala'a, G.M. Walker, S.J. Allen, M.N. Ahmad, Kinetic and thermodynamics of chromium ions adsorption onto low-cost dolomite adsorbent, Chem. Eng. J., 179 (2012) 193–202.
[26] J.F. Ji, Y. Ge, W.L. Balsam, J.E. Damuth, J. Chen, Rapid identification of dolomite using a Fourier transform infrared spectrophotometer (FTIR): a fast method for identifying Heinrich events in IODP Site U1308, Mar. Geol., 258 (2009) 60–68.
[27] J.H. Wang, X. Zhang, B. Zhang, Y.F. Zhao, R. Zhai, J.D. Liu, R.F. Chen, Rapid adsorption of Cr (VI) on modified halloysite nanotubes, Desalination, 259 (2010) 22–28.
[28] D. Ding, Y. Zhao, S. Yang, W. Shi, Z. Zhang, Z. Lei, Y. Yang, Adsorption of cesium from aqueous solution using agricultural residue walnut shell: equilibrium, kinetic and thermodynamic modeling studies, Water Res., 47 (2013) 2563–2571.
[29] H. Wang, Z.Z. Tian, L. Jiang, W.W. Luo, Z.G. Wei, S.Y. Li, J. Cui, W. Wei, Highly efficient adsorption of Cr(VI) from aqueous solution by Fe^{3+} impregnated biochar, J. Dispersion Sci. Technol., 38 (2017) 816–825.
[30] D. Wang, N. Chen, Y. Yang, W.W. Hu, C.P. Feng, Investigation on the adsorption of phosphorus by Fe-loaded ceramic adsorbent, J. Colloid Interface Sci., 464 (2016) 277–284.

[31] L. Zhou, Y.G. Liu, S.B. Liu, Y.C. Yin, G.M. Zeng, X.F. Tan, X. Hu, X.J. Hu, L.H. Jing, Y. Ding, S.H. Liu, X.X. Huang, Investigation of the adsorption-reduction mechanisms of hexavalent chromium by ramie biochar of different pyrolytic temperatures, Bioresour. Technol., 218 (2016) 351–359.
[32] F. Liu, X.H. Wang, B.Y. Chen, S.L. Zhou, C.T. Chang, Removal of Cr(VI) using polyacrylonitrile/ferrous chloride composite nanofibers, J. Taiwan Inst. Chem. Eng., 70 (2017) 401–410.
[33] N. Tewari, B.K. Guha, P. Vasudevan, Adsorption study of hexavalent chromium by bentonite clay, Asian J. Chem., 17 (2005) 2184–2190.
[34] S.S. Baral, S.N. Das, P. Rath, G.R. Chaudhury, Chromium(VI) removal by calcined bauxite, Biochem. Eng. J., 34 (2007) 69–75.
[35] G.X. Du, Z.H. Li, L.B. Liao, R. Hanson, S. Leick, N. Hoeppner, W.T. Jiang, Cr(VI) retention and transport through Fe(III)-coated natural zeolite, J. Hazard. Mater., 221–222 (2012) 118–123.
[36] B.S. Krishna, D.S.R. Murty, B.S.J. Prakash, Thermodynamics of chromium(VI) anionic species sorption onto surfactant-modified montmorillonite clay, J. Colloid Interface Sci., 299 (2000) 230–236.